Bioorganic & Medicinal Chemistry 20 (2012) 5592–5599

Contents lists available at SciVerse ScienceDirect

Bioorganic & Medicinal Chemistry

journal homepage: www.elsevier.com/locate/bmc

C-Glucosylated malonitrile as a key intermediate towards carbohydrate-based glycogen phosphorylase inhibitors

Sophie Feuillastre [a], Aikaterini S. Chajistamatiou [b], Constantinos Potamitis [b], Maria Zervou [b], Panagiotis Zoumpoulakis [b], Evangelia D. Chrysina [b,*], Jean-Pierre Praly [a,*], Sébastien Vidal [a,*]

[a] *Institut de Chimie et Biochimie Moléculaires et Supramoléculaires, Laboratoire de Chimie Organique 2 – Glycochimie, UMR 5246, CNRS, Université Claude Bernard Lyon 1, 43 Boulevard du 11 Novembre 1918, F-69622 Villeurbanne, France*

[b] *Institute of Biology, Medicinal Chemistry & Biotechnology, National Hellenic Research Foundation, 48 Vassileos Constantinou Avenue, Athens GR-11635, Greece*

ARTICLE INFO

Article history:
Received 12 March 2012
Revised 14 June 2012
Accepted 13 July 2012
Available online 2 August 2012

Keywords:
Carbohydrate
Glycogen phosphorylase
1,3-Dipolar cycloaddition
Malonitrile
Pyrimidinone

ABSTRACT

Glycogen utilization involves glycogen phosphorylase, an enzyme which appears to be a potential target for the regulation of glycaemia, as the liver isoform is a major player for hepatic glucose output. A single *C*-glucosylated malonitrile allowed for the synthesis of three glucose-based derivatives namely bis-oxadiazoles, bis-amides and a *C*-glucosylated tetrahydropyrimidin-2-one. When evaluated as glycogen phosphorylase inhibitors, two of the synthesized compounds displayed inhibition in the sub-millimolar range. In silico studies revealed that only one out of the bis-amides obtained and the *C*-glucosylated tetrahydropyrimidin-2-one may bind at the catalytic site.

1. Introduction

Control of hyperglycaemia is one of the major challenges in the prevention of type 2 diabetes complications. A large series of biological targets have been identified for the treatment of type 2 diabetes over the past decades[1–3] and glycogen phosphorylase[4] (GP) has been recognized as a possible macromolecular target for the control of hyperglycaemia.[1,5] This dimeric enzyme presents five different binding sites for a variety of small molecule inhibitors.[6–9] Glycogen phosphorylase inhibitors with high affinity for the catalytic site—the most extensively studied site of this enzyme—are mostly D-glucopyranose-based molecules with various substituents introduced at the anomeric position forming distinct classes.[6–10] The catalytic site of GP comprises a large cavity with high specificity for the D-glucopyranose moiety (Fig. 1) but also two additional pockets lying below and above the anomeric center of the carbohydrate moiety, that is, pointing into the α and β directions, respectively. Both subsites in the α and β directions have been explored with different substituents with the aim to identify the determinants of binding at this site.[5,6,9,10] Based on the well established homology between species and tissues isoforms of GP,[11] and because unphosphorylated GP (GP*b*) plays a crucial role in the reciprocal control between glycogenesis and glycogenolysis,[5–7] it is a common practice to use rabbit muscles GP*b* (RMGP*b*) for kinetic studies and inhibition evaluation.

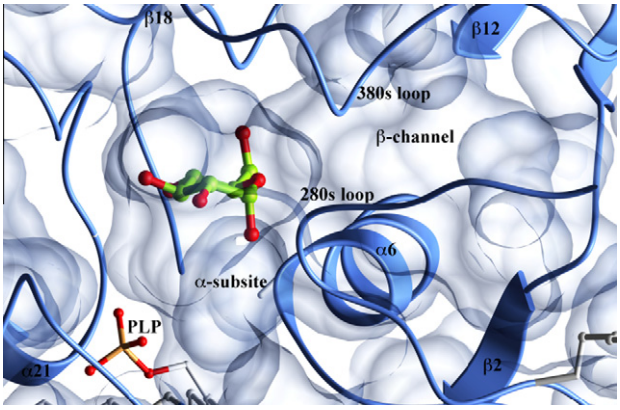

Figure 1. X-ray crystallographic structure of the catalytic site of GP (PDB code: 2PYD) in complex with α-D-glucopyranose and visualization of the α-subsite (below glucose and left to the 280s loop) and β-channel (on the right side of glucose and above the 280s loop).

Previous binding studies of GP in complex with potential inhibitors targeting the catalytic site revealed that the most potent ones had aromatic groups pointing towards the direction of β-pock-

* Corresponding authors. Tel.: +33 472 431 161; fax: +33 472 432 752 (J.-P.P.); tel.: +30 210 7273851; fax: +30 210 7273831 (E.D.C.).

E-mail addresses: echrysina@eie.gr (E.D. Chrysina), jean-pierre.praly@univ-lyon1.fr (J.-P. Praly).

0968-0896/$ - see front matter © 2012 Elsevier Ltd. All rights reserved.
http://dx.doi.org/10.1016/j.bmc.2012.07.033

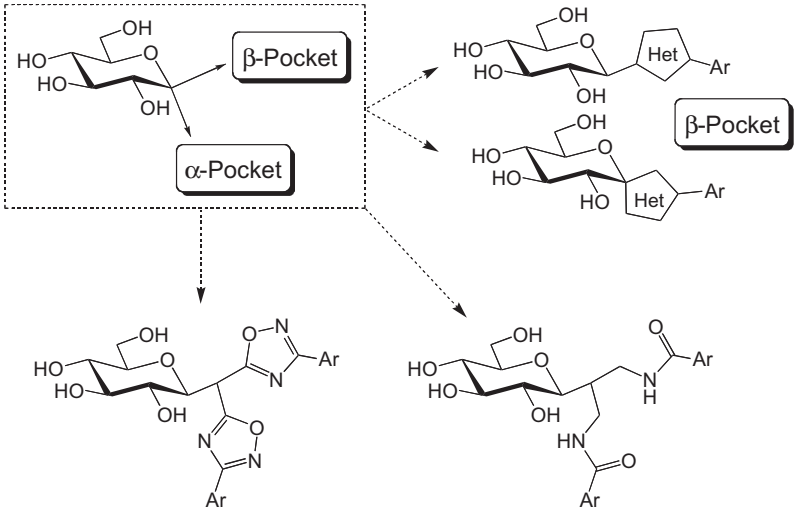

Figure 2. Structures of known (top right) and potential (bottom) GP inhibitors.

et.[7,12–20] The most suitable D-glucose-based scaffolds are substituted heterocycles with either a *C*-glucosidic bond or a spiro-bicyclic framework (Fig. 2). These structural designs provided potent inhibitors of GP with inhibition constants (K_i) in the low micromolar to sub-micromolar range. Such scaffolds improved the inhibitory potency of the ligands designed by taking advantage of the space occupied by water molecules in the β-channel and by forming additional contacts stabilizing the closed (inactive) conformation of the 280s loop. With the aim to make the most of both the unoccupied space and the 280s loop flexibility, a second aromatic moiety could be introduced in the vicinity of the anomeric position of the carbohydrate pointing towards the α-plane of the sugar (Fig. 2). The putative interactions of this additional substituent next to the anomeric center, with the residues lining the 280s loop of the enzyme could provide complementary contacts and strengthen binding, enhancing inhibitor potency. To this end, we have designed a general synthetic route from a *C*-glucosylated malonitrile precursor for the synthesis of bis-oxadiazole and bis-amide inhibitors as well as a *C*-glucosylated tetrahydropyrimidin-2-one.

2. Results and discussion

2.1. Synthesis of GP inhibitors

The *C*-glucosylated malonitrile precursor **2** was readily prepared according to a known procedure[21] from acetobromoglucose **1** and malonitrile (Scheme 1). The 1,3-dipolar cycloaddition with nitrile oxides, generated in situ from the corresponding α-chloroximes **3a**–**b**,[18] was then performed and provided the corresponding acetylated bis-oxadiazoles **4a**–**b** in good yields. Subsequent deacetylation afforded the desired hydroxylated *C*-glucosyl compounds **5a**–**b**. The moderate yields sometimes observed in these two syntheses were probably due to the acidity of the methine proton (H-α) between two electron withdrawing groups being either nitriles (for compound **2**) or 5-(1,2,4-oxadiazolyl) rings[13,18] (for compounds **4a**–**b**). The basic conditions applied for the 1,3-dipolar cycloaddition with in situ generation of nitrile oxides and/or the deacetylation step could lead to deprotonated intermediates prone to undergo ring-opening by cleavage of the endocyclic C–O bond and eventually formation of side products which were neither isolated nor characterized. The reduction of the *C*-glucosylated malo-

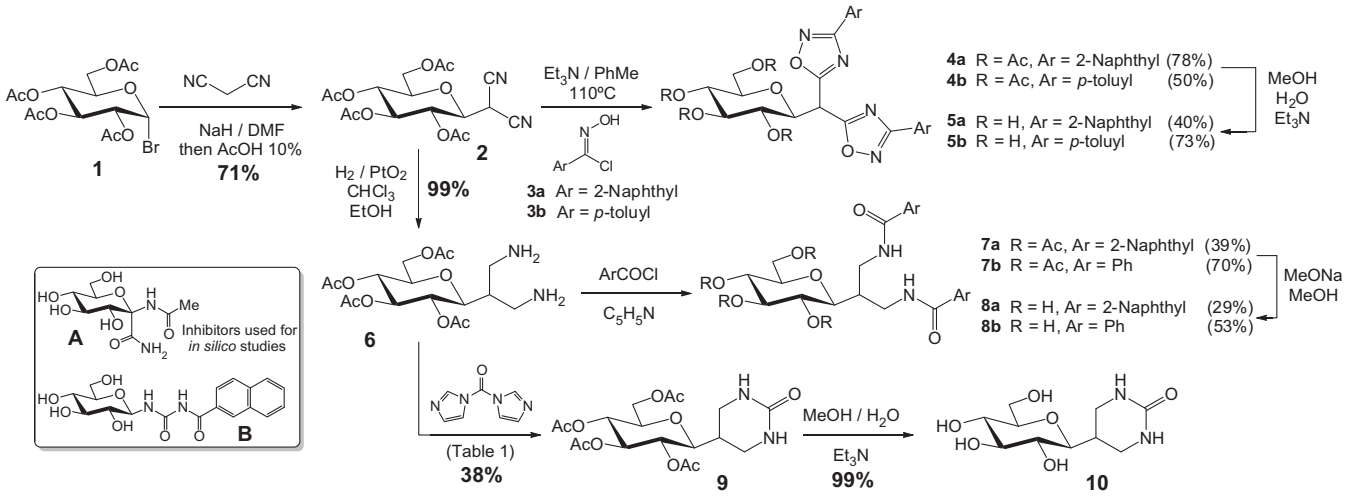

Scheme 1. Synthesis of the *C*-glucosylated bis-oxadiazoles **5a**–**b**, bis-amides **8a**–**b** and tetrahydropyrimidin-2-one **10** and structure of inhibitors **A**–**B** used for the in silico studies.

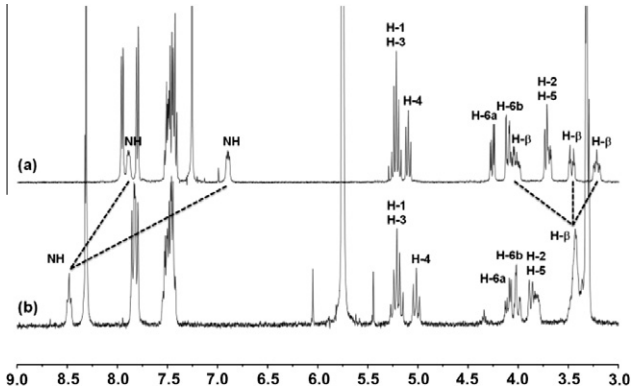

Figure 3. Partial ^{1}H NMR spectrum (293 K, 300 MHz) of acetylated bis-amide **7b** in (a) $CDCl_3$ and (b) DMSO-d_6.

nitrile **2** afforded the bis-amine **6**[21] (Scheme 1) and subsequent acylation provided the corresponding bis-amides **7a**–**b**. Deprotection under Zemplén conditions gave the hydroxylated bis-amides **8a**–**b** in high yields.

Interestingly, the ^{1}H NMR data collected for the acetylated bis-amide **7b** dissolved in $CDCl_3$ (Fig. 3a) displayed two signals for the NH protons (δ = 7.89 and 6.90 ppm). In addition, the signals of the methylene protons attached to the amide moieties (H-β) were also separated into three different signals: one multiplet (δ = 4.03) corresponding to two protons and two additional multiplets (δ = 3.47 and 3.22 ppm) for one proton each. The NMR spectrum recorded from a DMSO-d_6 solution (Fig. 3b) showed a single signal for both NH protons (δ = 8.50 ppm) and another signal resonating at δ = 3.45 ppm for the four methylene protons which merged into a single signal. Restricted rotation of the N–C(O) bond leading to separate amide rotamers being observable in the NMR time scale appears to be influenced by the medium. The hydrogen bond pattern could explain our observation as proposed in the model shown in Figure 4. The protons at position 2, 5 and 6 of the glucopyranosyl ring have their chemical shifts most affected by changing the solvent, while protons at positions 1, 3 and 4 are roughly unchanged (Fig. 3). In $CDCl_3$, this might be due to the formation of an intramolecular hydrogen bond between the NH protons and the oxygen atom of the carbonyl acetate at the 2 and/or 6 position of the carbohydrate (Fig. 4) thus creating either a 9- or a 11-membered ring between the glucose unit and the aglycon part. Another intramolecular hydrogen bond appears possible between one of the NH protons and the oxygen atom of the other amide moiety. This network of intramolecular interactions should entail restricted rotation in **7b**, thereby explaining the existence of several signals for the NH protons and for the methylene β-protons in $CDCl_3$, while in DMSO-d_6, intermolecular H-bonding between **7b** and the solvent should lead to more mobile species.

Finally, upon treatment with 1,1′-carbonyldiimidazole (CDI), the bis-amine **6** was converted into the tetrahydropyrimidin-2-one **9** that was deacetylated to afford the hydroxylated *C*-glucosyl derivative **10** (Scheme 1). Synthetic assays first attempted in DMF at 80 °C (Table 1, entry 1) afforded the desired tetrahydropyrimidin-2-one **9** in poor yield. The nucleophilicity of amines can be improved by using $AlMe_3$ to generate a highly nucleophilic aluminum–nitrogen complex with enhanced reactivity towards the addition to the carbonyl of CDI.[22] Moreover, the electrophilicity of the CDI carbonyl group can be enhanced by chelation with Lewis acids such as $AlMe_3$. Both of these possibilities most probably explain the better yield obtained when the reaction was performed in the presence of excess of $AlMe_3$ in refluxing dichloromethane (Table 1, entry 2). The formation of oligomers or polymers arising from the intermolecular addition of two amines from two different molecules of **6** might explain the limited improvement of the yield when the reaction was performed at 12 mM concentration of bis-amine **6**. In keeping with this hypothesis, the synthesis under diluted conditions afforded **9** in an acceptable 38% yield (1.2 mM, Table 1, entry 3).

2.2. Enzyme kinetics

The five glucose-based compounds **5a**–**b**, **8a**–**b** and **10** were evaluated for their potency as GP inhibitors (Table 2). Rabbit skeletal muscle glycogen phosphorylase *b* (RMGP*b*) was used as the model enzyme.[5–7] The bis-oxadiazole **5a** was poorly soluble in

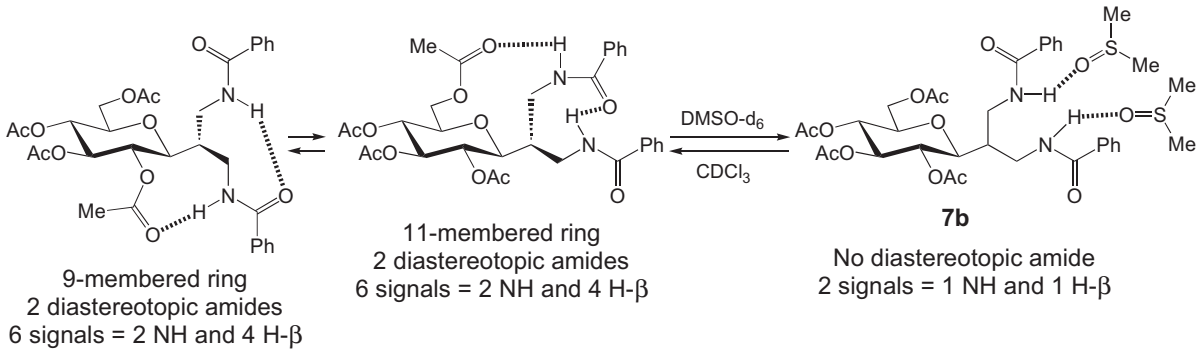

Figure 4. Possible H-bonded network for bis-amide **7b** influenced by the solvent used ($CDCl_3$ or DMSO-d_6).

Table 1
Synthesis of the tetrahydropyrimidin-2-one **9**

Entry	Reagents	Solvent	Concentration[a] (mM)	Temperature (°C)	Yield (%)
1	CDI	DMF	12	80	7
2	CDI/$AlMe_3$[b]	CH_2Cl_2	12	40	18
3	CDI/$AlMe_3$[b]	CH_2Cl_2	1.2	40	38

[a] Concentration of bis-amine **6**.
[b] CDI (1.1 equiv), $AlMe_3$ (3.5 equiv).

Table 2
Inhibition of RMGP*b* measured for the glucose-based compounds **5a–b**, **8a–b** and **10**

Compounds	Inhibition measured (μM)
5a	38% at 250[a]
5b	39% at 1000
8a	44% at 300
8b	21% at 1000
10	8.5% at 1000

[a] Partial solubility even in the presence of 20% DMSO in water; hence the inhibition is indicative and underestimated.

water even with 20% DMSO, as the two naphthyl groups present displaced the hydrophobic/hydrophilic balance towards highly hydrophobic properties. Therefore, the inhibitory potency described for compound **5a** might be slightly higher since only the supernatant of a saturated solution was used. Compounds **5b**, **8b** and **10** were poor inhibitors even at high concentration (1 mM). Nevertheless, the inhibition of RMGP*b* by the bis-naphthylamide **8a** is quite significant with 44% inhibition at 300 μM. Bis-oxadiazoles **5a–b** compare unfavorably to their related mono-oxadiazole counterparts, found from previous studies to exhibit both IC_{50} and K_i values in the low micromolar range[18] for the 2-naphthyl substituted compound. Both bulkiness and the presence of an additional carbon atom between the anomeric position and the oxadiazole rings could alter the binding of **5a–b** to the catalytic site of GP. Compared to some related *C*-glucopyranosyl pyrimidine nucleosides,[23,24] the *C*-glucosylated tetrahydropyrimidin-2-one **10** exhibited a much weaker inhibition against RMGP*b*.

2.3. Docking results

The binding mode of compounds listed in Table 2 was further investigated by in silico studies to account for the differences observed in their inhibitory potency. Our aim was also to comprehend better the unfavorable structural features in the vicinity of the anomeric center that would allow the rational design of improved inhibitors. Given the flexibility of the 280s loop and the structural dissimilarity among the studied compounds, two different crystal structures of RMGP*b* were used as starting models: (a) that found for RMGP*b* with the inhibitor *C*-(1-acetamido-α-D-glucopyranosyl) formamide (Scheme 1, **A**), bearing both α- and β-oriented substituents at the anomeric carbon atom and found to bind at the enzyme catalytic site (PDB code: 1P4H); (b) that found for RMGP*b* in complex with a bulkier inhibitor, 2-naphthoyl urea (Scheme 1, **B**) whose binding has already been associated with a shift of the 280s loop (residues 282–287).[9,25] The first model was used for the docking studies of compound **10** only. Our initial approach was to maintain the water network at the catalytic site. The docking procedure included the application of Glide XP with core constraint in order to 'lock' the glucopyranose moiety and subsequent redocking of the top ranked poses using QPLD-XP approach.[12,26] The docking protocol was validated using the x-ray crystal structures of both RMGP*b* complexes as well as a series of inhibitors with known binding affinities.[26]

2.3.1. Docking studies with 10 at the catalytic site of the formamide A/RMGPb complex

Results showed that compound **10** may bind at the active site of RMGP*b* in a way similar to the formamide **A** ligand (Fig. 5). The hydrogen bond interactions formed between the glucopyranose moiety and the residues of the catalytic site were maintained; namely, His377:O6, Asn484:O6, Gly675:O4, Asn484:O4, Ser674:O3, Glu672:O3, Glu672:O2 and a water-mediated hydrogen bond between O4 and Thr676. No additional electrostatic interaction was observed for the pyrimidinone ring. Furthermore, an unfavorable van der Waals interaction (4.18 kcal mol^{-1}) was observed due to the close contact of the pyrimidone ring with the side chain of Asn284. The corresponding interaction in RMGP*b*-formamide docked complex though, is energetically favorable (−2.16 kcal mol^{-1}). The absence of electrostatic interactions (apart from the glucose ring) coupled with the presence of unfavorable van der Waals interactions may provide an explanation for the low inhibition of enzyme activity by compound **10** (8.5% at 1000 μM).

2.3.2. Docking studies at the catalytic site of 2-naphthoyl urea B/RMGPb complex

The most prominent changes in the 2-naphthoyl urea/RMGP*b* complex structure involve the distal arrangement of Asn284 and the loss of the close contact formed between the side chain atoms of Asn284 with O2 of the sugar coupled with dislocation of Phe285. These changes result in creating a wider cavity for ligand binding. Docking of the voluminous compounds **5a**, **5b**, **8a**, **8b** failed to report any poses in the binding pocket of 2-naphthoyl urea **B**/RMGP*b* complex. Compound **10** was also tested for docking at the catalytic site of this complex. Avoiding the steric clashes with the 280s loop, the synthesized molecule could bind in a similar mode with the 2-naphthoyl urea derivative **B** at the catalytic site of RMGP*b* but its pyrimidinone ring failed again to develop any additional electrostatic interaction (data not shown).

In order to investigate whether the bulkier compounds **5a**, **5b**, **8a** and **8b** could dock in a less hindered pocket, all the 415 water

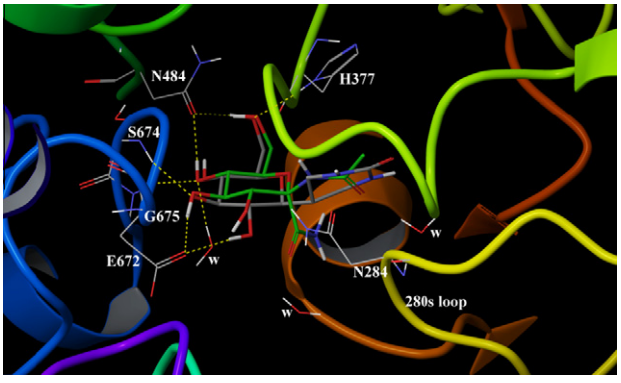

Figure 5. The best docked pose of **10** (shown in grey) at the catalytic site of the formamide **A**/RMGP*b* complex (PDB code: 1P4H) superimposed onto formamide **A** (shown in green). Direct and water-mediated hydrogen bond interactions of **10** with the residues lining the binding site are depicted in dotted lines.

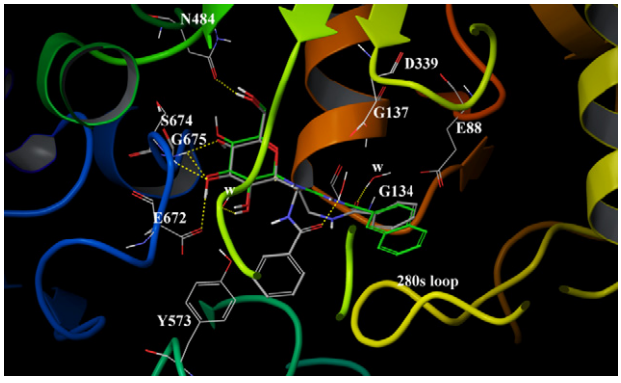

Figure 6. The best docked pose of **8b** (shown in grey) at the catalytic site of the modified 2-naphthoyl urea **B**/RMGP*b* complex (in the absence of five water molecules) superimposed onto 2-naphthoyl urea (shown in green). Hydrogen bond interactions of **8b** with the residues lining the binding site are depicted in dotted lines.

molecules of the 2-naphthoyl urea/RMGP*b* complex structure were excluded. This approach resulted in acceptable docking poses that maintained the position of glucopyranose moiety only for **8b**. Moreover, one of its side chains (β branch) was oriented towards the β-channel and smoothly overlaid the 2-naphthoyl urea moiety of compound **B**, while the other chain (α-like branch) laid on a plane parallel to the glucose ring.

To further explore the role of the solvent structure, the water molecules that hindered the binding of **8b** at the catalytic site of RMGP*b*, were identified by inspecting the **8b** docked pose in the absence of all water molecules. Then, the RMGP*b* crystal structure was subjected to a stepwise deletion of five water molecules, lying in close proximity to the α-like branch of **8b**, leading to its successful binding at the catalytic site (Fig. 6). Comparison of QPLD-XP docking results for **8b** with the crystal structure of the complex with 2-naphthoyl urea **B** showed that crucial hydrogen bonding interactions between the glucopyranose moiety and the residues of the catalytic site are maintained; namely, Asn484:O6, Gly675:O4, Gly675:O3, Ser674:O3 and Glu672:O3. Further to this, **8b** specific binding features are the loss of two hydrogen bonds between His377:O6 and Asn484:O4 as well as between two water molecules and O2 (one of the water molecules has been deleted). In addition, both carbonyl groups of **8b** side chains form water-mediated electrostatic interactions with residues in the vicinity (β branch carbonyl group with Glu88, Gly134, Gly137 and α-like branch carbonyl group with Asp339). Furthermore, the conformation adopted by α-like branch is induced by the π–π interactions between **8b** phenyl group and Tyr573.

Application of MM-GBSA post docking scoring protocol calculated a ΔG_{bind} of −124.4 kcal mol^{-1} for **8b**. The corresponding free energy value for 2-naphthoyl urea **B** in the absence of the same water molecules was ΔG_{bind} = −102.8 kcal mol^{-1} (compared to ΔG_{bind} = −130.5 kcal mol^{-1} when all waters were included). This difference could be attributed to the lack of several favorable electrostatic interactions, induced by the disruption of a stable water network, involving loss of crucial water interactions with O2 of glucopyranose as well as with the amide groups of the urea moiety. MM-GBSA binding site strain energy calculation, upon deletion of the aforementioned five water molecules, gave an increased value by 13 kcal mol^{-1} as compared to the strain energy when all water molecules were present. This could be an indication that the catalytic site is in a thermodynamically less favorable state after water deletion, which possibly accounts for the reduced inhibitory potency of **8b** (21% at 1000 μM).

Additional efforts to accommodate compounds **5a**, **5b** and **8a** at the catalytic site involved docking studies with induced flexibility of the receptor (IFD protocol). No favorable results were obtained for none of the compounds since the geometry had to be considerably distorted to get accommodated to the catalytic site. Since this finding is not in accordance with the kinetic results obtained for **8a**, it suggests that there might be weak binding of this compound at a different RMGP*b* site.

3. Conclusion

Short routes to potential glycogen phosphorylase inhibitors were designed from a *C*-glucosylated malonitrile precursor. 1,3-Dipolar cycloaddition with nitrile oxides provided the corresponding bis-oxadiazoles, while reduction of the nitrile moieties afforded a bis-amine, and subsequently bis-amides, by *N*-acylation. 1,1′-Carbonyldiimidazole reacted with the bis-amine in the presence of trimethylaluminium and under diluted conditions so as to form a tetrahydropyrimidin-2-one derivative by cyclization. Five inhibitors were obtained and their inhibition towards RMGP*b* was evaluated. The enzymatic data attested to poor inhibitory properties towards RMGP*b* with two of the compounds responding in the sub-millimolar range concentration. In silico studies indicated that **10** may bind at the catalytic site; however, the unfavorable van der Waals interactions identified with Asn284 of the formamide **A**/RMGP*b* complex binding site might account for the poor inhibition observed. In the case of the branched compound **8b**, theoretical calculations showed that it could be accomodated at the wider binding site of the 2-naphthoyl urea **B**/RMGP*b* complex. Binding of **8b** seems to require disruption of the solvent network and concomitant loss of interactions stabilizing the complex that could possibly explain the weak inhibition. The slightly improved inhibitory potency of **8a** taking into account that it failed to be accommodated at the catalytic site might be attributed to binding at a different site of RMGP*b*. In the absence of structural evidence, the poor inhibition observed for all compounds synthesized to target the catalytic site could be interpreted in terms of the limited space in the vicinity of the α-subsite and steric hindrance induced by bulky substituents. Despite the unsatisfactory potency exhibited, the docking results of these molecules could provide guiding information in a structure-based inhibitor design approach.

4. Experimental section

4.1. General methods

All reagents and solvents used for syntheses were commercial and used without further purification. Solvents were distilled over CaH_2 (CH_2Cl_2), Mg/I_2 (MeOH), or purchased dry. Reactions were performed under argon atmosphere. NMR spectra were recorded at 293 K, unless stated otherwise, using a 300, 400 or 500 MHz spectrometer. Shifts are referenced relative to deuterated solvent residual peaks. Low and high resolution mass spectra were recorded in the positive mode using a Bruker MicroTOF-Q II XL spectrometer. Thin-layer chromatography (TLC) was carried out on aluminum sheets coated with silica gel 60 F_{254} (Merck). TLC plates were inspected by UV light (λ = 254 nm) and developed by treatment with a solution of 10% H_2SO_4 in EtOH/H_2O (1:1 v/v) or $KMnO_4$ in H_2O or ninhydrin in *n*-BuOH/H_2O followed by heating. Silica gel column chromatography was performed with silica gel Si 60 (40–63 μm). Optical rotations were measured using a Perkin Elmer polarimeter and values are given in deg dm^{-1} g^{-1} cm^3.

4.2. General procedure A for 1,3-dipolar cycloaddition

A solution of *C*-glucosyl malonitrile **2** (0.25 mmol) and hydroximoyl chloride **3a**–**b**[18] (2.2 mmol, 9 equiv) in toluene (10 mL) was stirred at 110 °C under argon. Triethylamine (1.3 mmol, 5 equiv) was dissolved in toluene (1 mL) and slowly added over 12 h with a syringe pump. The solvent was evaporated to dryness. The residue was purified by flash silica gel column chromatography (EtOAc/PE 3:7) to afford the desired bis-oxadiazoles **4a**–**b**.

4.3. General procedure B for deacetylation of bis-oxadiazoles

A solution of the acyl-protected bis-oxadiazoles **4a**–**b** (0.2 mmol) in MeOH (7 mL), extra pure water (1.5 mL) and triethylamine (1.5 mL) was stirred at room temperature for 3 days. The solution was then evaporated to dryness and the residue was purified by flash silica gel column chromatography (CH_2Cl_2/MeOH 9:1) to afford the hydroxylated bis-oxadiazoles **5a**–**b**.

4.4. General procedure C for preparation of bis-amides

A solution of bis-amine **6** (0.2 mmol) and aryl chloride (0.48 mmol, 4 equiv) in dry pyridine (5 mL) was stirred at room

temperature during 2 h. The reaction was then poured into EtOAc (50 mL) and the organic layer was washed with HCl 1 N (2 × 35 mL), saturated $NaHCO_3$ (2 × 35 mL) and saturated NaCl (35 mL), dried ($MgSO_4$), filtered and evaporated to dryness. The residue was purified by flash silica gel column chromatography (EtOAc/PE 3:7 to EtOAc).

4.5. General procedure D for Zemplén deacylation

A solution of the acyl-protected carbohydrate derivatives **7a**–**b** or **9** (0.05 mmol) and MeONa (0.025 mmol, 0.5 equiv) in a solution of freshly distilled MeOH (1 mL) and CH_2Cl_2 (5 mL) was stirred at room temperature for 2 days. The solution was then evaporated to dryness and the residue was purified by C-18 reverse-phase chromatography (H_2O/CH_3CN 5:5) to afford the desired hydroxylated products.

4.6. 2-(2,3,4,6-Tetra-*O*-acetyl-β-D-glucopyranosyl)-malonitrile (2)[21]

To a solution of malonitrile (1.2 g, 18.3 mmol, 5 equiv) in DMF (6 mL) was added NaH (0.51 g, 21.2 mmol, 5.8 equiv) by portions. After gas evolution ceased, 2,3,4,6-tetra-*O*-acetyl-α-D-glucopyranosyl bromide **1** (1.5 g, 3.65 mmol) in DMF (3 mL) was added dropwise at 0 °C. The reaction mixture was stirred for 2 h at 0 °C and then 10% aqueous AcOH (60 mL) was added and the solution was stirred overnight at room temperature. The precipitate was collected, then dissolved in CH_2Cl_2, dried ($MgSO_4$) and evaporated to dryness to obtain **2** (1.02 g, 71%) as a white foam. R_f = 0.13 (PE/EtOAc 7:3). ^{1}H NMR (300 MHz, $CDCl_3$): δ (ppm) = 5.29 (dd, 1H, J = 9.2, 9.5 Hz, H-3), 5.17 (dd, 1H, J = 9.5, 9.5 Hz, H-4), 5.14 (dd, 1H, J = 9.2, 9.2 Hz, H-2), 4.28 (dd, 1H, J = 4.9, 12.5 Hz, H-6a), 4.18 (dd, 1H, J = 2.4, 12.5 Hz, H-6b), 4.02 (d, 1H, J = 4.3 Hz, H-α), 3.97 (dd, 1H, J = 4.3, 9.2 Hz, H-1), 3.86 (ddd, J = 2.4, 4.9, 9.5 Hz, 1H, H-5), 2.12, 2.11, 2.06, 2.04 (4s, 12H, $COCH_3$). ^{13}C NMR (100 MHz, $CDCl_3$): δ (ppm) = 172.7, 172.2, 170.7, 170.2 (4s, *C*OCH_3), 109.1 (s, 2C, C≡N), 77.4 (C-5), 74.7 (C-1), 73.1 (C-3), 70.0 (C-4), 67.6 (C-2), 61.5 (C-6), 26.9 (C-α), 21.2, 20.8, 20.7 (3s, 4C, CH_3).

4.7. (2,3,4,6-Tetra-*O*-acetyl-β-D-glucopyranosyl)-di-[3-(2-naphthyl)-1,2,4-oxadiazol-5-yl]methane (4a)

Prepared according to the general procedure **A** from **2** (100 mg, 0.25 mmol) to afford **4a** (145.1 mg, 78%) as a brown oil. R_f = 0.65 (PE/EtOAc 7:3). $[\alpha]_D^{20}$ −3.0 (c = 1.00, $CHCl_3$). ^{1}H NMR (400 MHz, $CDCl_3$): δ (ppm) = 8.65 (s, 2H, H-ar), 8.14 (d, 2H, J = 8.5 Hz, H-ar), 7.97-7.88 (m, 6H, H-ar), 7.59-7.55 (m, 4H, H-ar), 5.37 (dd, 1H, J = 9.2, 9.6 Hz, H-2), 5.30 (dd, 1H, J = 9.1, 9.2 Hz, H-3), 5.25 (d, 1H, J = 7.2 Hz, H-α), 5.12 (dd, 1H, J = 9.5, 9.7 Hz, H-4), 4.76 (dd, 1H, J = 7.2, 9.6 Hz, H-1), 4.13 (dd, 1H, J = 5.9, 12.3 Hz, H-6a), 4.04 (dd, 1H, J = 2.2, 12.3 Hz, H-6b), 3.87 (ddd, 1H, J = 2.2, 5.9, 9.5 Hz, H-5), 2.04, 1.99, 1.87, 1.77 (4s, 12H, $COCH_3$). ^{13}C NMR (100 MHz, $CDCl_3$): δ (ppm) = 172.5, 172.3 (2s, C-5-oxa), 170.6, 170.4 (2s, C-3-oxa), 169.5, 169.2, 169.1, 169.0 (4s, *C*OCH_3), 135.0, 134.9, 133.1 (3s, 6C, C^{IV}-ar), 129.1, 129.07, 129.01, 128.6, 128.5, 128.05, 128.04, 127.98, 127.86, 127.07, 126.99, 123.83, 123.75 (13s, 14C, CH-ar), 77.4 (C-5), 76.7 (C-1), 74.2 (C-3), 71.0 (C-2), 68.4 (C-4), 62.0 (C-6), 40.8 (C-α), 20.4, 20.6, 20.7, 22.8 (CH_3). HR-ESI-MS (positive mode): m/z Calcd for $C_{39}H_{35}N_4O_{11}$ $[M+H]^+$ 735.2297. Found 735.2273.

4.8. (2,3,4,6-Tetra-*O*-acetyl-β-D-glucopyranosyl)-di-[3-(*p*-tolyl)-1,2,4-oxadiazol-5-yl]methane (4b)

Prepared according to general procedure **A** from **2** (250 mg, 0.63 mmol) to afford **4b** (211.5 mg, 50%) as a brown oil. R_f = 0.40 (PE/EtOAc 7:3). $[\alpha]_D^{20}$ −7.4 (c = 0.50, $CHCl_3$). ^{1}H NMR (400 MHz, $CDCl_3$): δ (ppm) = 7.97 (d, 4H, J = 8.3 Hz, H-ar), 7.29 (dd, 4H, J = 3.5, 8.3 Hz, H-ar), 5.34 (dd, 1H, J = 9.2, 9.6 Hz, H-2), 5.25 (dd, 1H, J = 9.2, 9.6 Hz, H-3), 5.14 (d, 1H, J = 7.2 Hz, H-α), 5.08 (dd, 1H, J = 9.5, 9.6 Hz, H-4), 4.67 (dd, 1H, J = 7.2, 9.6 Hz, H-1), 4.11 (dd, 1H, J = 5.9, 12.3 Hz, H-6a), 4.01 (dd, 1H, J = 2.3, 12.3 Hz, H-6b), 3.82 (ddd, 1H, J = 2.3, 5.9, 9.5 Hz, H-5), 2.42 (s, 6H, Ph*Me*), 2.02, 1.97, 1.88, 1.74 (4s, 12H, $COCH_3$). ^{13}C NMR (100 MHz, $CDCl_3$): δ (ppm) = 172.5, 172.4 (2s, C-5-oxa), 171.0, 170.7, 169.8, 169.4 (4s, *C*OCH_3), 142.6, 142.4 (2s, C-3-oxa), 130.2, 130.1, 130.0 (3s, 4C, CH-ar), 123.8 (1s, 2C, C^{IV}-ar), 77.7 (C-5), 77.0 (C-1), 74.6 (C-3), 71.2 (C-2), 68.7 (C-4), 62.3 (C-6), 41.0 (C-α), 22.1 (1s, 2C, Ph*Me*), 21.5, 21.0, 20.9, 20.6 (CH_3). HR-ESI-MS (positive mode): m/z Calcd for $C_{33}H_{35}N_4O_{11}$ $[M+H]^+$ 663.2299. Found 663.2297.

4.9. (β-D-Glucopyranosyl)-di-[3-(2-naphthyl)-1,2,4-oxadiazol-5-yl)]methane (5a)

Prepared according to general procedure **B** from **4a** (145 mg, 0.19 mmol) to afford **5a** (44.4 mg, 40%) as a beige foam. R_f = 0.20 (CH_2Cl_2/MeOH 9:1). $[\alpha]_D^{20}$ = +3.6 (c = 1.00, CH_3OH). ^{1}H NMR (400 MHz, CD_3OD): δ (ppm) = 8.66 (s, 2H, H-ar), 8.13 (m, 2H, H-ar), 8.02-7.98 (m, 6H, H-ar), 7.58 (m, 4H, H-ar), 4.41 (d, 1H, J = 9.6 Hz, H-α), 3.80 (dd, 1H, J = 2.1, 12.2 Hz, H-6a), 3.63 (dd, 1H, J = 5.6, 12.2 Hz, H-6b), 3.56 (dd, 1H, J = 9.0, 9.6 Hz, H-1), 3.48 (dd, 1H, J = 8.8, 9.0 Hz, H-2), 3.43 (ddd, 1H, J = 2.1, 5.6, 9.5 Hz, H-5), 3.33-3.28 (m overlap with CD_3OD, 2H, H-3, H-4). ^{13}C NMR (100 MHz, CD_3OD): δ (ppm) = 176.0, 175.3 (2s, C-5-oxa), 170.0 (1s, 2C, C-3-oxa), 136.2, 134.5, 128.89 (3s, 6C, C^{IV}-ar), 130.0, 129.94, 129.89, 129.2, 128.9, 128.1, 128.0, 124.6 (8s, 14C, CH-ar), 82.3 (C-5), 79.8 (C-α), 79.4 (C-2), 73.0 (C-1), 71.2 (C-3 or C-4), 62.4 (C-6), 48.8 (C-3 or C-4). HR-ESI-MS (positive mode): m/z Calcd for $C_{31}H_{27}N_4O_7$ $[M+H]^+$ 567.1874. Found 567.1890.

4.10. (β-D-Glucopyranosyl)-di-[3-(*p*-tolyl)-1,2,4-oxadiazol-5-yl]methane (5b)

Prepared according to general procedure **B** from **4b** (200 mg, 0.30 mmol) to afford **5b** (109 mg, 73%) as a beige foam. R_f = 0.70 (CH_2Cl_2/MeOH 9:1). $[\alpha]_D^{20}$ −1.4 (c = 0.5, CH_3OH). ^{1}H NMR (400 MHz, CD_3OD): δ (ppm) = 7.96 (dd, 4H, J = 2.4, 8.0 Hz, H-ar), 7.34 (dd, 4H, J = 4.3, 8.0 Hz, H-ar), 5.51 (d, 1H, J = 4.6 Hz, H-α), 4.32 (dd, 1H, J = 4.6, 9.3 Hz, H-1), 3.76 (dd, 1H, J = 2.2, 12.2 Hz, H-6a), 3.59 (dd, 1H, J = 5.6, 12.2 Hz, H-6b), 3.46 (m, 2H, H-2, H-3), 3.38 (ddd, 1H, J = 2.2, 5.6, 9.6 Hz, H-5), 3.27 (m overlap with CD_3OD, 1H, H-4), 2.41 (d, 6H, J = 1.4 Hz, Ph*Me*). ^{13}C NMR (100 MHz, CD_3OD): δ (ppm) = 169.81, 169.78 (2s, C-5-oxa), 143.4, 143.3 (2s, C-3-oxa), 130.73, 130.70, 128.4 (3s, 4C, CH-ar), 124.9, 124.8 (2s, C^{IV}-ar), 82.5 (C-5), 79.9 (C-1), 79.6 (C-3), 73.2 (C-2), 71.4 (C-4), 62.7 (C-6), 41.2 (C-α), 21.5 (1s, 2C, Ph*Me*). HR-ESI-MS (positive mode): m/z Calcd for $C_{25}H_{26}N_4NaO_7$ $[M+Na]^+$ 517.1694. Found 517.1670.

4.11. 2-(2,3,4,6-Tetra-*O*-acetyl-β-D-glucopyranosyl)-1,3-diaminopropane (6)[21]

Compound **2** (50 mg, 0.13 mmol) and PtO_2 (14 mg, 0.06 mmol, 0.5 equiv) were suspended in ethanol (25 mL) and $CHCl_3$ (5 mL) and the suspension was stirred vigorously under H_2 atmosphere (1 atm.) overnight. The catalyst was filtered off over celite then the filtrate was evaporated to dryness to afford compound **6** as a white foam (61.5 mg, 99%). ^{1}H NMR (300 MHz, CD_3OD): δ (ppm) = 5.31 (dd, 1H, J = 9.3, 9.3 Hz, H-3), 5.14 (m, 2H, H-2, H-4), 4.30 (dd, 1H, J = 5.4, 12.6 Hz, H-6a), 4.21 (dd, 1H, J = 2.4, 12.6 Hz, H-6b), 3.92 (m, 2H, H-1, H-5), 3.32-3.22 (m overlap with CD_3OD, 1H, H-β), 2.31 (br s, 1H, H-α), 2.11, 2.07, 2.03, 2.00 (4s, 12H, $COCH_3$).

4.12. 2-(2,3,4,6-Tetra-*O*-acetyl-β-D-glucopyranosyl)-1,3-di-(2-naphthamido)propane (7a)

Prepared according to general procedure **C** from **6** (50 mg, 0.12 mmol) and 2-naphthoyl chloride (92 mg, 0.48 mmol) to afford **7a** (33.5 mg, 39%) as a white foam. R_f = 0.05 (EtOAc/PE 3:7). $[\alpha]_D^{20}$ = +8.7 (*c* = 0.6, $CHCl_3$). ^{1}H NMR (400 MHz, $CDCl_3$): δ (ppm) = 8.53 (s, 1H, H-ar), 8.36 (s, 1H, H-ar), 8.15 (m, 1H, NH), 8.00 (dd, 2H, *J* = 8.0, 25.7 Hz, H-ar), 7.89 (m, 7H, H-ar), 7.57(m, 3H, H-ar), 7.14 (m, 1H, NH), 5.25 (m, 2H, H-2, H-3), 5.12 (m, 1H, H-4), 4.31 (m, 1H, H-6a), 4.17 (m, 1H, H-6b), 3.77 (m, 1H, H-1), 3.72 (m, 1H, H-5), 4.12, 3.57, 3.34 (3 m, 4H, H-β), 2.13 (m overlap with OAc signals, 1H, H-α), 2.16, 2.10, 2.07, 2.01 (4s, 12H, $COCH_3$). ^{13}C NMR (100 MHz, $CDCl_3$): δ (ppm) = 170.7, 170.4, 170.3, 169.7 (4s, *C*OCH_3), 168.7, 167.7 (2s, CONH), 135.0, 132.9, 132.8, 131.5, 131.3 (5s, 6C, C^{IV}-ar), 129.3, 129.1, 128.64, 128.55, 128.1, 128.0, 127.9, 127.8, 127.7, 127.0, 126.7, 123.8, 123.3 (13s, 14C, CH-ar), 80.2 (C-1), 76.5 (C-5), 74.3 (C-3), 69.4 (C-2), 68.3 (C-4), 62.3 (C-6), 39.0 (C-α), 36.2, 40.2 (2s, C-β), 20.9, 20.8, 20.7 (3s, 4C, CH_3). HR-ESI-MS (positive mode): *m*/*z* Calcd for $C_{39}H_{41}N_2O_{11}$ $[M+H]^+$ 713.2705. Found 713.2704.

4.13. 2-(2,3,4,6-Tetra-*O*-acetyl-β-D-glucopyranosyl)-1,3-dibenzamidopropane (7b)

Prepared according to general procedure **C** from **6** (50 mg, 0.12 mmol) and benzoyl chloride (56 μL, 0.48 mmol) to afford **7b** (51.5 mg, 70%) as a white foam. R_f = 0.76 (EtOAc). $[\alpha]_D^{20}$ −3.8 (*c* = 0.4, $CHCl_3$). ^{1}H NMR (400 MHz, $CDCl_3$): δ (ppm) = 7.95 (m, 2H, H-ar), 7.89 (m, 1H, NH), 7.80 (m, 2H, H-ar), 7.48 (m, 6H, H-ar), 6.90 (m, 1H, NH), 5.20 (m, 2H, H-1, H-3), 5.10 (m, 1H, H-4), 4.26 (dd, 1H, *J* = 4.8, 12.5 Hz, H-6a), 4.11 (m, 1H, H-6b), 3.73 (m, 1H, H-2), 3.69 (ddd, 1H, *J* = 4.8, 7.1, 9.9 Hz, H-5), 4.03, 3.47, 3.22 (3 m, 4H, H-β), 2.10 (m overlap with OAc signals, 1H, H-α), 2.09, 2.05, 2.02, 1.95 (4s, 12H, $COCH_3$). ^{13}C NMR (100 MHz, $CDCl_3$): δ (ppm) = 170.7, 170.33, 170.30, 169.7 (4s, *C*OCH_3), 168.7, 167.7 (2s, CONH), 134.3, 134.2 (2s, C^{IV}-ar), 132.0, 131.7, 128.8, 128.7, 127.3, 127.0 (6s, 10C, CH-ar), 80.3 (C-2), 76.4 (C-5), 74.3 (C-3), 69.4 (C-1), 68.3 (C-4), 62.3 (C-6), 38.7 (C-α), 35.9, 39.6 (2s, C-β), 20.7, 20.8, 20.9 (3s, 4C, CH_3). HR-ESI-MS (positive mode): *m*/*z* Calcd for $C_{31}H_{37}N_2O_{11}$ $[M+H]^+$ 613.2392. Found 613.2385.

4.14. 2-(β-D-Glucopyranosyl)-1,3-di-(2-naphthamido)propane (8a)

Prepared according to general procedure **D** from **7a** (33.5 mg, 0.05 mmol) to afford **8a** (7.3 mg, 29%) as a white foam. R_f = 0.90 (CH_2Cl_2/MeOH/$H_2$0 4:6:0.5). $[\alpha]_D^{20}$ = +5.8 (*c* = 0.14, CH_3OH). ^{1}H NMR (400 MHz, CD_3OD): δ (ppm) = 8.41 (d, 2H, *J* = 4.9 Hz, H-ar), 7.94 (m, 8H, H-ar), 7.56 (m, 4H, H-ar), 3.94 (d, 1H, *J* = 11.3 Hz, H-6a), 3.84 (m, 2H, H-β), 3.70 (m, 2H, H-β, H-6b), 3.59 (dd, 1H, *J* = 7.1, 14.1 Hz, H-β), 3.53 (m, 2H, H-1 or H-2 or H-3 or H-4 or H-5), 3.37 (m overlap with CD_3OD, 3H, H-1 or H-2 or H-3 or H-4 or H-5), 2.61 (m, 1H, H-α). ^{13}C NMR (100 MHz, CD_3OD): δ (ppm) = 170.5 (1s, 2C, CONH), 136.3, 134.1, 132.8 (3s, 6C, C^{IV}-ar), 130.09, 130.05, 129.4, 129.2, 128.82, 128.80, 128.75, 127.8, 124.9 (9s, 14C, CH-ar), 82.3, 81.2, 80.1, 72.3, 71.8 (5s, C-1, C-2, C-3, C-4, C-5), 61.1 (C-6), 39.7 (C-α), 41.5, 34.9 (2s, C-β). HR-ESI-MS (positive mode): *m*/*z* Calcd for $C_{31}H_{33}N_2O_7$ $[M+H]^+$ 545.2282. Found 545.2280.

4.15. 1,3-Dibenzamido-2-(β-D-glucopyranosyl)propane (8b)

Prepared according to general procedure **D** from **7b** (50 mg, 0.08 mmol) to afford **8b** (7.5 mg, 53%) as a white foam. R_f = 0.85 (CH_2Cl_2/MeOH/$H_2$0 4:6:0.5). $[\alpha]_D^{20}$ −6.7 (*c* = 0.34, CH_3OH). ^{1}H NMR (400 MHz, CD_3OD): δ (ppm) = 7.86 (m, 4H, H-ar), 7.49 (m, 6H, H-ar), 3.89 (m, 1H, H-6a), 3.75, 3.70, 3.65 (3 m, 3H, H-6, H-β), 3.58 (dd, 1H, *J* = 6.0, 13.7 Hz, H-β), 3.50, 3.47, 3.43 (3 m, 3H, H-1 or H-2 or H-3 or H-4, H-β), 3.35 (m overlap with CD_3OD, 2H, H-1 or H-2 or H-3 or H-4), 3.28 (m overlap with CD_3OD, 1H, H-5), 2.51 (m, 1H, H-α). ^{13}C NMR (100 MHz, CD_3OD): δ (ppm) = 170.5, 170.4 (2s, CONH), 135.6 (1s, 2C, C^{IV}-ar), 132.7, 129.6, 128.3 (3s, 10C, CH-ar), 82.2 (C-5), 81.0, 80.1, 72.3, 71.8 (4s, C-1, C-2, C-3, C-4), 63.1 (C-6), 39.7 (C-α), 41.1, 38.2 (2s, C-β). HR-ESI-MS (positive mode): *m*/*z* Calcd for $C_{23}H_{29}N_2O_7$ $[M+H]^+$ 445.1965. Found 445.1965.

4.16. 5-(2,3,4,6-Tetra-*O*-acetyl-β-D-glucopyranosyl)tetrahydropyrimidin-2(1*H*)-one (9)

A solution of bis-amine **6** (50 mg, 0.12 mmol) in freshly distilled CH_2Cl_2 (100 mL) was cooled at 0 °C. Then, $AlMe_3$ (0.42 mmol, 3.5 equiv) was added slowly at 0 °C and the mixture was stirred during 15 min. 1,1′-Carbonyldiimidazole (0.13 mmol, 1.1 equiv) diluted in CH_2Cl_2 (2 mL) was then added at room temperature and the mixture was stirred at 45 °C overnight. Water (50 mL) was added slowly at room temperature and the aqueous layer was extracted with CH_2Cl_2 (3 × 150 mL). The organic layers were combined, washed with saturated NaCl (5 × 30 mL), dried ($MgSO_4$), filtered and evaporated to dryness. The residue was purified by flash silica gel column chromatography (EtOAc/MeOH 9:1) to give compound **9** as a white foam (21 mg, 38%). R_f = 0.21 (EtOAc/MeOH 85:15). $[\alpha]_D^{20}$ −13.0 (*c* = 0.4, $CHCl_3$). ^{1}H NMR (400 MHz, $CDCl_3$): δ (ppm) = 5.23 (br s, 1H, NH), 5.18 (dd, 1H, *J* = 9.2, 9.6 Hz, H-3), 4.99 (m, 2H, H-2, H-4), 4.93 (br s, 1H, NH), 4.18 (dd, 1H, *J* = 2.3, 9.9 Hz, H-6a), 4.08 (dd, 1H, *J* = 5.0, 9.9 Hz, H-6b), 3.61 (ddd, 1H, *J* = 2.3, 5.0, 9.9 Hz, H-5), 3.52 (m, 1H, H-1), 3.37 (m, 2H, H-β), 3.20 (m, 2H, H-β), 2.11 (m overlap with OAc signals, 1H, H-α), 2.10, 2.07, 2.04, 2.03 (4s, 12H, $COCH_3$). ^{13}C NMR (100 MHz, $CDCl_3$): δ (ppm) = 170.7, 169.6 (2s, 4C, *C*OCH_3), 156.8 (NHCONH), 76.6 (C-1), 76.2 (C-5), 74.4 (C-3), 69.6 (C-2), 68.4 (C-4), 62.2 (C-6), 42.7, 39.5 (2s, C-β), 32.6 (C-α), 20.9, 20.7 (2s, 4C, CH_3). HR-ESI-MS (positive mode): *m*/*z* Calcd for $C_{18}H_{27}N_2O_{10}$ $[M+H]^+$ 431.1660. Found 431.1663.

4.17. 5-(β-D-Glucopyranosyl)tetrahydropyrimidin-2(1*H*)-one (10)

Prepared according to general procedure **D** from **9** (10 mg, 0.02 mmol) to afford **10** (6 mg, 99%) as a white foam. R_f = 0.66 (CH_2Cl_2/MeOH/H_2O 6:4:0.5). $[\alpha]_D^{20}$ −0.5 (*c* = 0.2, CH_3OH). ^{1}H NMR (500 MHz, CD_3OD): δ (ppm) = 3.82 (dd, 1H, *J* = 1.9, 12.0 Hz, H-6a), 3.60 (dd, 1H, *J* = 5.5, 12.0 Hz, H-6b), 3.42 (m, 1H, H-β), 3.33 (m, 2H, H-β, H-1 or H-2 or H-3 or H-4 or H-5), 3.29 (m, 2H, H-β), 3.19 (m, 4H, H-1 or H-2 or H-3 or H-4 or H-5), 2.34 (m, 1H, H-α). ^{13}C NMR (125 MHz, CD_3OD): δ (ppm) = 159.7 (C=O), 82.0, 80.0, 79.6, 73.2, 71.7 (5s, C-1, C-2, C-3, C-4, C-5), 63.1 (C-6), 43.6, 40.7 (2s, C-β), 34.1 (C-α). HR-ESI-MS (positive mode): *m*/*z* Calcd for $C_{10}H_{19}N_2O_6$ $[M+H]^+$ 263.1238. Found 263.1235.

4.18. Determination of inhibition of RMGP*b*

RMGP*b* was isolated from rabbit skeletal muscle according to Fischer & Krebs,[27] using 2-mercaptoethanol. Kinetic experiments at different inhibitor concentrations were conducted in the direction of glycogen synthesis, at 30 °C in the presence of 2 mM glucose-1-phosphate (G-1-P) and 1 mM AMP. The phosphate released was calculated with Fiske & Subbarow[28] and Saheki, Takeda & Shimazu[29] methods.

4.19. Docking calculations

In silico studies were performed using SCHRÖDINGER Suite 2011.[30] The crystal structure of RMGP*b* in complex with the *C*-(1-

acetamido-α-D-glucopyranosyl) formamide **A** (PDB code: 1P4H) was initially selected as a starting model. The protein was pre-treated using Protein Preparation Wizard. Water molecules lying at a distance beyond 5 Å of the ligand were deleted. Bond orders were assigned, hydrogens were added and assigned with an exhaustive sampling including water orientations. The system was optimized with minimization procedure using convergence criterion RMSD of 0.3 Å to heavy atoms (Force field OPLS2005). The crystal structure of RMGP*b* in complex with the inhibitor 2-naphthoyl urea **B**[9,25] was subsequently used as an initial model in which the 280s loop is subjected to extended shifts to allow binding of bulkier ligands at the catalytic site. The protein was pre-treated as previously described maintaining all the water molecules. Docking calculations were performed using GLIDE module (v. 5.7) in extra-precision (XP) mode. Core constraint was applied on the ligand to 'lock' the glucopyranose ring atoms. Best docking poses were re-docked by applying quantum polarized ligand docking procedure (QPLD-XP). The post docking scoring approach MM-GBSA of the Prime module (v. 3.0) was then applied for the theoretical calculation of ΔG_{bind} indicating the ligand/binding site interaction energy of the complex and the strain energy of the binding site.

Acknowledgments

Financial supports from CNRS, University Claude-Bernard Lyon 1 and the French Agence Nationale de Recherche (project GPdia N° ANR-08-BLAN-0305) are gratefully acknowledged. This work was supported by the FP7 Capacities coordination and support actions REGPOT-2008-1-No 230146 'EUROSTRUCT' and REGPOT-2009-1-No 245866 'ARCADE'. Dr. F. Albrieux, C. Duchamp and N. Henriques are gratefully acknowledged for mass spectrometry analyses.

Supplementary data

Supplementary data (^{1}H and ^{13}C NMR spectra for compounds **2**, **4a**–**b**, **5a**–**b**, **6**, **7a**–**b**, **8a**–**b**, **9** and **10**) associated with this article can be found, in the online version, at http://dx.doi.org/10.1016/j.bmc.2012.07.033.

References and notes

1. Agius, L. *Best Pract. Res. Clin. Endocrinol. Metab.* **2007**, *21*, 587.
2. Moller, D. E. *Nature* **2001**, *414*, 821.
3. Ross, S. A.; Gulve, E. A.; Wang, M. *Chem. Rev.* **2004**, *104*, 1255.
4. Newgard, C. B.; Hwang, P. K.; Fletterick, R. J. *Crit. Rev. Biochem. Mol. Biol.* **1989**, *24*, 69.
5. Oikonomakos, N. G. *Curr. Prot. Pept. Sci.* **2002**, *3*, 561.
6. Oikonomakos, N. G.; Somsák, L. *Curr. Opin. Invest. Drugs* **2008**, *9*, 379.
7. Praly, J.-P.; Vidal, S. *Mini-Rev. Med. Chem.* **2010**, *10*, 1102.
8. Somsák, L. C. R. *Chimie* **2011**, *14*, 211.
9. Somsák, L.; Czifrák, K.; Tóth, M.; Bokor, E.; Chrysina, E. D.; Alexacou, K. M.; Hayes, J. M.; Tiraidis, C.; Lazoura, E.; Leonidas, D. D.; Zographos, S. E.; Oikonomakos, N. G. *Curr. Med. Chem.* **2008**, *15*, 2933.
10. Watson, K. A.; Mitchell, E. P.; Johnson, L. N.; Bichard, C. J. F.; Orchard, M. G.; Fleet, G. W. J.; Oikonomakos, N. G.; Leonidas, D. D.; Son, J. C. *Biochemistry* **1994**, *33*, 5745.
11. Newgard, C. B.; Nakano, K.; Hwang, P. K.; Fletterick, R. J. *Proc. Natl. Acad. Sci. U.S.A.* **1986**, *83*, 8132.
12. Benltifa, M.; Hayes, J. M.; Vidal, S.; Gueyrard, D.; Goekjian, P. G.; Praly, J.-P.; Kizilis, G.; Tiraidis, C.; Alexacou, K.-M.; Chrysina, E. D.; Zographos, S. E.; Leonidas, D. D.; Archontis, G.; Oikonomakos, N. G. *Bioorg. Med. Chem.* **2009**, *17*, 7368.
13. Benltifa, M.; Vidal, S.; Fenet, B.; Msaddek, M.; Goekjian, P. G.; Praly, J.-P.; Brunyánszki, A.; Docsa, T.; Gergely, P. *Eur. J. Org. Chem.* **2006**, 4242.
14. Benltifa, M.; Vidal, S.; Gueyrard, D.; Goekjian, P. G.; Msaddek, M.; Praly, J.-P. *Tetrahedron Lett.* **2006**, *47*, 6143.
15. Bertus, P.; Szymoniak, J.; Jeanneau, E.; Docsa, T.; Gergely, P.; Praly, J.-P.; Vidal, S. *Bioorg. Med. Chem. Lett.* **2008**, *18*, 4774.
16. Cecioni, S.; Argintaru, O.-A.; Docsa, T.; Gergely, P.; Praly, J.-P.; Vidal, S. *New J. Chem.* **2009**, *33*, 148.
17. He, L.; Zhang, Y. Z.; Tanoh, M.; Chen, G.-R.; Praly, J.-P.; Chrysina, E. D.; Tiraidis, C.; Kosmopoulou, M. N.; Leonidas, D. D.; Oikonomakos, N. G. *Eur. J. Org. Chem.* **2007**, 596.
18. Nagy, V.; Benltifa, M.; Vidal, S.; Berzsényi, E.; Teilhet, C.; Czifrák, K.; Batta, G.; Docsa, T.; Gergely, P.; Somsák, L.; Praly, J.-P. *Bioorg. Med. Chem.* **2009**, *17*, 5696.
19. Praly, J.-P.; He, L.; Qin, B. B.; Tanoh, M.; Chen, G.-R. *Tetrahedron Lett.* **2005**, *46*, 7081.
20. Tóth, M.; Kun, S.; Bokor, É.; Benltifa, M.; Tallec, G.; Vidal, S.; Docsa, T.; Gergely, P.; Somsák, L.; Praly, J.-P. *Bioorg. Med. Chem.* **2009**, *17*, 4773.
21. Inaba, Y.; Fujimoto, T.; Ono, H.; Obata, M.; Yano, S.; Mikata, Y. *Carbohydr. Res.* **2008**, *343*, 941.
22. Lee, S.-H.; Matsushita, H.; Clapham, B.; Janda, K. D. *Tetrahedron* **2004**, *60*, 3439.
23. Gimisis, T. *Mini-Rev. Med. Chem.* **2010**, *10*, 1127.
24. Tsirkone, V. G.; Tsoukala, E.; Lamprakis, C.; Manta, S.; Hayes, J. M.; Skamnaki, V. T.; Drakou, C.; Zographos, S. E.; Komiotis, D.; Leonidas, D. D. *Bioorg. Med. Chem.* **2010**, *18*, 3413.
25. Nagy, V.; Felfoldi, N.; Konya, B.; Praly, J.-P.; Docsa, T.; Gergely, P.; Chrysina, E. D.; Tiraidis, C.; Kosmopoulou, M. N.; Alexacou, K.-M.; Konstantakaki, M.; Leonidas, D. D.; Zographos, S. E.; Oikonomakos, N. G.; Kozmon, S.; Tvaroska, I.; Somsak, L. *Bioorg. Med. Chem.* **2012**, *20*, 1801.
26. Hayes, J. M.; Leonidas, D. D. *Mini-Rev. Med. Chem.* **2010**, *10*, 1156.
27. Fischer, E. H.; Krebs, E. G.; Sidney, P. C.; Kaplan, N. O. *Methods Enzymol.* **1962**, *5*, 369.
28. Fiske, C. H.; Subbarow, Y. *J. Biol. Chem.* **1925**, *66*, 375.
29. Saheki, S.; Takeda, A.; Shimazu, T. *Anal. Biochem.* **1985**, *148*, 277.
30. Schrödinger Suite 2011, LLC: New York, NY, 2011.